

Preparation, Characterization, and Catalytic Activity of Silica-Supported Highly Dispersed Pt-Fe Catalysts

L. GUCZI, K. MATUSEK AND M. ESZTERLE

*Institute of Isotopes of the Hungarian Academy of Sciences,
P.O. Box 77, H-1525 Budapest, Hungary*

Received March 29, 1978; revised December 19, 1978

The catalytic and surface properties of highly dispersed Pt-Fe catalyst supported on SiO₂ have been investigated by Mössbauer spectroscopy, chemisorption, isotope exchange, and hydrogenolysis of ethane and *n*-butane. At low iron concentration Mössbauer spectra indicate Pt-Fe formation and at the same time an increase in the adsorption of H₂, O₂, and CO. A parallelism between adsorption properties and catalytic activity can be interpreted by an increase in the number of surface metal atoms as a result of Pt-Fe formation. This is supported by the constancy of activation energy and the selectivity change in the reaction of *n*-butane hydrogenolysis. At higher iron loading iron is enriched on the surface to some extent and the reaction parameters mentioned are characteristic of iron itself, i.e., activity and activation energies decreased. Since the activity of Pt-Fe/SiO₂ is still higher by about three orders of magnitude than that of iron alone it is assumed that the activation of iron requires Pt neighbors by which either hydrogen can be supplied to iron sites or iron can be "diluted" thus retarding the deactivation process. These results are supported by the selectivity data.

1. INTRODUCTION

In the current renaissance of alloy catalysis much effort has been made to elucidate the interaction between Group VIII and Group IB metals (1-3). It is considerably more difficult to study the interaction between two transition metals because, beside the *geometric* effect, the electron interaction, e.g., the *ligand* effect, cannot be neglected (4).

Of the possible transition metal combinations only a few attempts have been made to characterize the Pt-Fe system. Bartholomew and Boudart (5) have used Mössbauer spectroscopy and chemisorption in their exploratory work. They have established the formation of the Pt-Fe alloy in carbon-supported Pt-Fe catalyst, and no enrichment in the surface phase in the whole concentration range has been observed. Garten and Ollis (6) have given

further evidence for the alloy phase by studying Pd-Fe supported on alumina. Garten (7) has observed the formation of the Pt-Fe phase on SiO₂ support and at low iron concentration he has found surface enrichment in iron arising from the effect of oxygen at high temperature. This could be eliminated by repeated hydrogen treatment.

On the other hand, Engels and co-workers (8, 9) have observed the formation of a superstructure phase, Pt₃Fe, for nonsupported platinum-iron alloy in the concentration range between 10 and 15 atom% iron using X-ray diffraction. The increase in hydrogen and CO adsorption measured in this concentration range of iron was correlated to smaller particle size due to the superstructure phase. The same effect was assumed to be operative for the Pt-Fe catalyst supported on alumina

TABLE 1
Catalyst Preparation

Catalyst	Description of preparation
A	1.1 wt% Pt in form of $\text{Pt}(\text{NH}_3)_4(\text{OH})_2$ on SiO_2
B	As A plus acidic treatment at $\text{pH} \cong 1$
C	As B plus 0.1 wt% Fe in form of $\text{Fe}(\text{NO}_3)_3$ in water
D	As B plus 0.2 wt% Fe in form of $\text{Fe}(\text{NO}_3)_3$ in water
E	As B plus 0.7 wt% Fe in form of $\text{Fe}(\text{NO}_3)_3$ in water
F	Physical mixture of $\text{Pt}(\text{NH}_3)_4/\text{SiO}_2$ and $\text{Fe}(\text{NO}_3)_3/\text{SiO}_2$
G	0.5 wt% Fe on SiO_2 at $\text{pH} = 1$

although direct measurement of particle size was not possible

Catalytic reactions were carried out only in two cases. The activity of the Pt-Fe alloy, as well as Pt-Fe/ η - Al_2O_3 , increased for ethane hydrogenolysis at 15.5 and 10.8 atom% Fe, respectively, which was due to the increase in Pt dispersion (10). On the contrary, in the Pt-Fe/ γ - Al_2O_3 system the change in the selectivity of the CO/ H_2 synthesis reaction was interpreted by electron drift from iron to platinum; consequently, iron was inactivated in Pt-Fe clusters (11).

In view of the controversial data we decided to study the supported Pt-Fe system further. In order to avoid a large interaction between the metallic phase and the support, we have used silica gel as support because both alumina and carbon supports are considered to have great influence on the metals (12), and thus it seems difficult to draw any definite conclusion regarding the catalytic effect of the bimetallic system itself. In this way the disturbance caused by the hydrogen spillover effect being operative mainly on alumina and on charcoal may be avoided. The structure of the catalyst surface has been studied by TG-MS, Mössbauer spectroscopy, and chemisorption, and the catalytic activity has been investigated by deuterium exchange and hydrogenolysis of ethane and *n*-butane.

2. EXPERIMENTAL

$\text{Pt}(\text{NH}_3)_4^{2+}$ ions were exchanged with the surface OH groups of silica gel (SAS,

specific surface area 560 m^2/g) to prepare Pt/ SiO_2 catalysts by the method of Benesi *et al.* (13). In Table 1 experimental conditions for the preparation of bimetallic catalysts are presented. In all cases the catalyst was dried at 393 K overnight followed by a 1-hr treatment in oxygen at 573 K and 3-hr reduction in a stream of hydrogen at 773 K. This procedure is considered to be standard treatment.

The different elementary steps of the catalyst preparation prior to reduction were followed by TG-MS as detailed elsewhere (14).

The behavior of the bimetallic Pt-Fe/ SiO_2 formed after the standard treatment was studied by Mössbauer spectroscopy (15). A $^{57}\text{Co}/\text{Cr}$ source was driven in the constant acceleration mode and a multi-channel analyzer was used to record the spectra. For calibration stainless steel sheet enriched in ^{57}Fe was applied. Mössbauer data were submitted to a least-square analysis using a Mössbauer fitting program.

All adsorption measurements were carried out in a dynamic apparatus using, alternately, helium and nitrogen as carrier gas.

Temperature programmed desorption of hydrogen (TPD) was carried out after hydrogen treatment at 873 K followed by cooling the sample in hydrogen atmosphere to room temperature.

Hydrogenolysis of ethane and *n*-butane was studied in a circulating apparatus which was connected to a Varian 1400 gas chromatograph. A 1-m long column filled with alumina was applied to separate reaction products using a temperature range between 333 and 423 K. Between the catalytic runs the catalysts were treated by oxygen at 1 kPa followed by reduction in 30-kPa hydrogen at the reaction temperature. A stable catalytic activity was revealed after this treatment. Hydrogen-deuterium exchange was measured using an MS 10 C2 mass spectrometer. Data on a direct correlation between exchange

and hydrogenolysis were obtained with a DuPont 21-490 gas chromatograph-mass spectrometer.

The metal concentration on SiO_2 was determined by X-ray fluorescence.

3. RESULTS

3.1. Catalyst Preparation and Characterization

In contrast to the data reported earlier (13) the exchange between $\text{Pt}(\text{NH}_3)_4^{2+}$ and surface hydroxyl group results at room temperature in the deposition of half the amount of platinum from a 20-ml solution containing 5.6×10^3 mol liter⁻¹ Pt. Catalyst *A* was obtained from this platinum tetrammine complex on silica by standard treatment.

Bimetallic catalysts were produced by impregnation of $\text{Pt}(\text{NH}_3)_4^{2+}/\text{SiO}_2$ dried overnight at 393 K with $\text{Fe}(\text{NO}_3)_3$ solution at pH = 1 (catalysts *C*, *D*, and *E*). The acidic treatment with HNO_3 was necessary to avoid the precipitation of ferric hydroxide during the drying process. The effect of this treatment itself on catalytic activity was studied by a catalyst (denoted by *B*) prepared by acid treatment of $\text{Pt}(\text{NH}_3)_4^{2+}$ on silica at pH = 1.

To check the formation of the bimetallic system a physical mixture of $\text{Pt}(\text{NH}_3)_4^{2+}/\text{SiO}_2$ and $\text{Fe}(\text{NO}_3)_3/\text{SiO}_2$ was prepared (catalyst *F*) with the final concentration of 1.1 wt% Pt and 0.7 wt% Fe. Catalyst *G* was prepared by impregnation with 0.5 wt% $\text{Fe}(\text{NO}_3)_3$ solution of pH = 1.

The formation of the bimetallic system was investigated prior to and after a calcination-reduction procedure. TG-MS measurements on catalysts *A*, *D*, and *E* detailed elsewhere (14) showed that the platinum tetrammine complex is bonded to the silica gel surface via the formation of Pt-O-Si bonds. The fixation of this complex results in a relatively high dispersion (see later). When silica gel contains both the complex and ferric nitrate the

TABLE 2
Mössbauer Parameters of Fe-Pt/SiO₂ Catalysts with Different Iron Loads^a

	Fe content (atom%)	δ (mm/sec)	Δ (mm/sec)	Γ (mm/sec)	$\frac{dx^2}{df}$
C	26.0	0.30 ± 0.09	0.41	0.67	2.07
D	41.0	0.34 ± 0.05	0.51	0.71	1.11
E	71.0	0 ± 0.12	0.0	0.63	2.22

^a Calculation: (E, F) asymmetric doublet at $\Gamma_1 = \Gamma_2$; (G) single peak.

decomposition of this mixture in an argon atmosphere indicates an interaction between these two substances. Ammonia is partly oxidized by nitrate ions resulting in the formation of N_2O , N_2 , and H_2O but only small amount of NO which is the main decomposition product from $\text{Fe}(\text{NO}_3)_3$. Argon atmosphere, as distinct from oxidizing conditions as in the calcination, was necessary to study the fine structure of this interaction, thereby avoiding the total oxidation of nitrogen compounds to NO_2 .

The catalyst obtained after standard treatment was studied by Mössbauer spectroscopy using 0.6-mg ⁵⁷Fe with 88% enrichment in a 300-mg sample. Essentially, in the case of catalysts *C* and *D* a broad, non-Lorentzian peak due to superparamagnetism (small particle size) and to the distribution of iron environment can be obtained. The isomer shift and quadrupole splitting can be calculated by fitting the curve with the asymmetric constrained doublet as presented in Table 2 (for details see Ref. (15)).

These values are in good agreement with the δ values measured for Pt-Fe/carbon (5) and Pt-Fe/ γ -Al₂O₃ (11).

The formation of Pt-Fe on silica gel is strongly supported by the observation that previously oxidized iron can be reduced by hydrogen at room temperature.

At high iron loading two peaks can be observed. The calculation of the spectra obtained for catalyst *E* with the constrained doublet of Fe^{2+} and Fe^{3+} produces

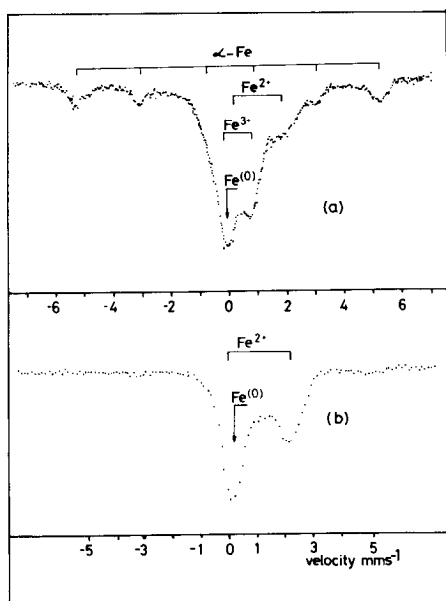


FIG. 1. Fe/SiO₂ reduced at 973 K, prepared by impregnation at (a) pH = 3 and (b) pH = 1.

a singlet the isomer shift of which is characteristic of iron alone (see Table 2).

The basic difference between catalysts with low and high iron content is that in the latter case a fraction of Fe³⁺ above Fe/Pt = 1 cannot be reduced even at high temperature (15). Although here the isomer shift predicts the presence of only Fe⁰ on the surface, we may assume also the existence of Pt-Fe because all iron oxidized can be converted back to Fe⁰ by hydrogen at room temperature. Nevertheless, the isomer shift is sensitive only to the first sphere of neighborhood of iron thus al-

lowing us to infer the presence of Pt-Fe clusters, the amount of which is so small that it cannot be resolved in the spectrum.

The effect of platinum on the Mössbauer spectrum of iron is further proved if the catalyst G, Fe/SiO₂, is studied. In Fig. 1 Mössbauer spectra of two types of iron catalysts are presented. Curve (a) shows the catalyst prepared by impregnation at pH = 3, curve (b) the one deposited at pH = 1. The reduction temperature in both cases was 973 K, which is 200 K higher than used for platinum containing catalysts. For the sample prepared at pH = 3 a small amount of iron can be formed in large crystallites with only a small degree of reduction. The Fe/SiO₂ impregnated at pH = 1 appears in small crystallites and due to this only two species, paramagnetic iron and Fe²⁺ appear in the spectrum. Moreover, neither of these resembles the spectrum of catalyst E and regardless of the state of dispersion the oxidized sample cannot be reduced in hydrogen at room temperature.

3.2. Adsorption and TPD Measurements

Since all samples were amorphous to X-ray diffraction, hydrogen, oxygen, and CO adsorption as well as hydrogen titration were applied to characterize these catalysts.

Table 3 presents the chemisorption results. Due to the ambiguity in stoichiometry for oxygen-hydrogen titration (16)

TABLE 3
Adsorption Data on Pt-Fe/SiO₂ Catalysts

Catalyst	Fe (atom%)	Amount adsorbed (μmol/g _{cat})			O ₂ -H ₂ titration H ₂ (μmol/g _{cat})	O ₂ irreversible (μmol/g _{cat})
		O ₂	H ₂	CO		
A	0	9.6	12.9	17.9	31.7	0
B	0	5.7	9.8	12.9	21.9	0
C	26.0	9	13.8	18.7	28.2	0
D	41.0	6.7	6.3	8.6	18.0	1.1
E	71.0	5.2	2.1	2.7	4.9	3.6
G	100.0	9	—	—	—	9

H/Pt and CO/Pt ratios were first determined by taking $O/Pt = 1$. The experimental data for H/Pt and CO/Pt are 1.37 and 0.96, respectively, and the H/O ratios calculated by the adsorption and that obtained by titration are 3.29 and 3.21, respectively.

All data summarized in the table are obtained on catalysts which have been stabilized by reaction. These values are somewhat lower than those measured on fresh catalysts.

Good agreement can be found between oxygen and CO adsorption, whereas hydrogen uptake is somewhat higher on all catalysts. Nevertheless, these data give a rough approximation of the effects on the surface metal concentration caused by the different treatments and by alloying.

A comparison of catalysts *A* and *B* shows that there is a small drop in the number of surface Pt atoms (the loss of platinum content is negligible as indicated by X-ray fluorescence method). Since the platinum complex is attached to the surface by Pt-O-Si bonds these might be broken on acidic treatment. As a consequence, the Pt complex may migrate on the surface to form larger crystallites with the simultaneous drop in metallic dispersion. Under the effect of a small amount of iron addition the adsorption of all gases used increases (compare *B* and *C*). The extent of this change is nearly the same, so we may assume that the adsorption stoichiometry is not largely affected by alloying of platinum with iron. Moreover, chemisorbed oxygen can be reversibly reduced at room temperature and thus the enhanced adsorption is probably due to an increase in the concentration of surface metal atoms.

On further iron addition the adsorption of all gases decreases but hydrogen and CO adsorption drops to a larger extent than the total oxygen uptake at room temperature. Some of these oxygen atoms, however, are reversibly bonded to the

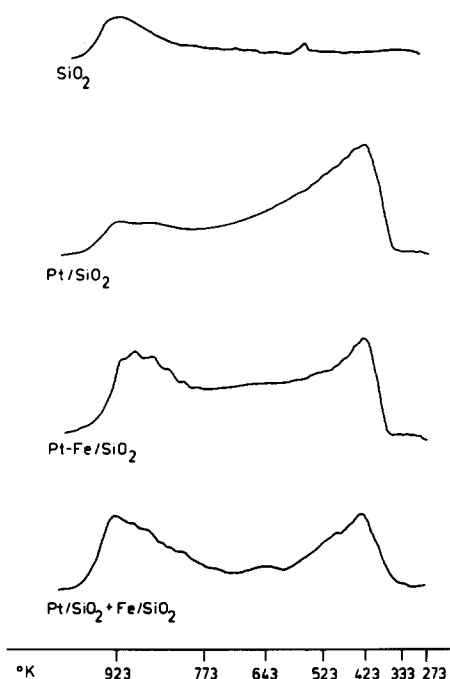


FIG. 2. TPD measurements (a) on silica alone; (b), (c), (d), on catalysts *A*, *D*, and *F*, respectively.

metal and can easily be removed by hydrogen, as is shown in column 7 of Table 3. The metallic phase holding the reversible fraction of oxygen must be Pt-Fe and not Pt alone since a part of the Fe^{3+} is also reduced to Fe^0 at room temperature, as has been shown by Mössbauer data (15).

The physical mixture (catalyst *F*) very much resembles pure platinum in its adsorption properties, and it is therefore not included in the table. The lack of measurable hydrogen and CO chemisorption on Fe/SiO_2 at room temperature is difficult to understand. In the literature a reduced adsorption of these gases has also been observed (8, 9). At high temperature, however, hydrogen can be adsorbed, as is shown from TPD measurements.

TPD measurement has been applied to elucidate the influence of iron addition on the hydrogen adsorption. Figure 2 shows the desorption of hydrogen from SiO_2 alone, and from catalysts *A*, *D*, and *G*.

On pure Pt/SiO_2 all the hydrogen can be removed at around 423 K whereas on

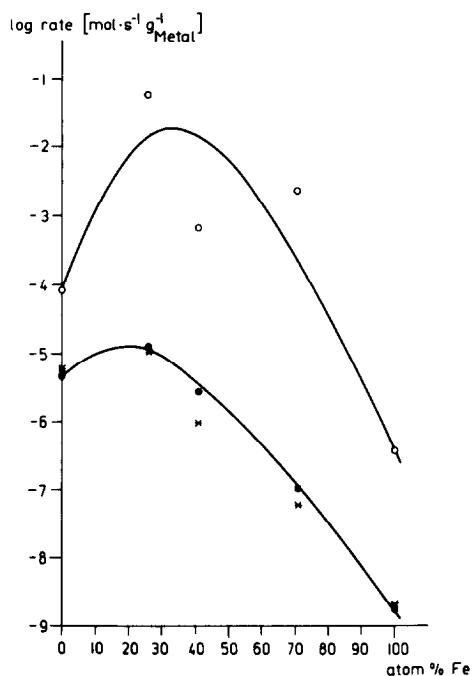


Fig. 3. Catalytic activity for ethane exchange (○) at 473 K, for ethane hydrogenolysis (×) at 573 K, and *n*-butane hydrogenolysis (●) at 523 K, vs Fe content.

Pt-Fe a part of the hydrogen is not readily available and desorbs only at about 923 K. When just iron on silica is studied, no hydrogen can be desorbed up to 673 K. When TPD is carried out after room temperature adsorption on Fe/SiO₂ no hydrogen can be recovered, which means that hydrogen uptake on Fe/SiO₂ occurs only after high-temperature activation. This behavior resembles that found by Yao and Shelef (17) for supported rhenium catalyst. The physical mixture behaves as if both iron and platinum were on the surface separately.

3.3. Catalytic Reactions

Catalytic activities for deuterium exchange in ethane measured in the temperature range between 380 K and 621 K as well as for hydrogenolysis of ethane (temperature interval 525 to 831 K) and butane (temperature interval 466 to 837 K)

are presented in Fig. 3. The activities are referred to the unit weight of metal because the determination of surface metal atoms for the bimetallic system by chemisorption involves uncertainties. The catalytic activity curves pass through a maximum at about 25 atom% iron content. The rate of ethane exchange is always higher in the whole iron concentration range than that of ethane hydrogenolysis. This was observed when ethane hydrogenolysis was carried out in the presence of deuterium. At 383 K the deuterium content of ethane reaches equilibrium after 2-min contact time whereas hydrogenolysis commences only above 473 K.

The activation energy was determined with a standard 1:10 hydrocarbon-hydrogen mixture. These data are presented in Fig. 4 and show that with increasing iron content the activation energy for both hydrogenolyses falls, indicating that at higher concentration iron exerts a definite influence on the hydrogenolysis. This is supported by the reaction order w.r.t. hydrogen which is shown for ethane and *n*-butane in Figs. 5 and 6, respectively. The activation energy and hydrogen order

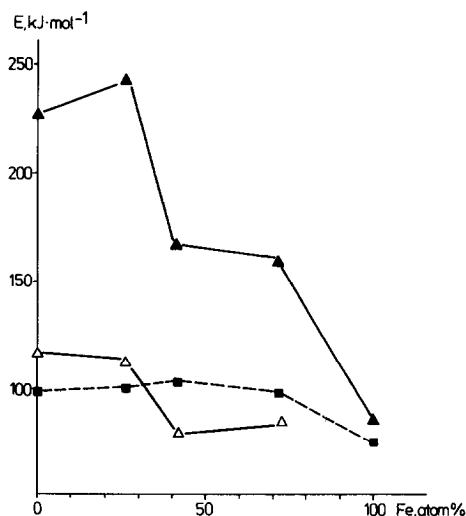


Fig. 4. Activation energy vs Fe content: (■), ethane exchange; (▲), ethane hydrogenolysis; (△), butane hydrogenolysis.

measured on a physical mixture of Pt/SiO₂ and Fe/SiO₂ are close to those obtained for Pt/SiO₂. The dotted vertical lines indicate the hydrogen pressure in the standard mixture. In both cases the hydrogen order increases, which again points to a change in the character of the bimetallic catalyst with respect to Pt/SiO₂.

Analysis of selectivity pattern for *n*-butane hydrogenolysis reveals the fine structure of the iron effect. Comparing the pattern characteristic of pure Pt/SiO₂ with that shown on platinum black (18), the main difference is the preferential formation of ethane due to the rupture at the middle C-C bond. Ethane selectivity on Pt/SiO₂ increases with increasing temperature and with decreasing hydrogen pressure, but similar to that which emerged on platinum black, at high hydrogen pressure and at low activity, statistical C-C bond cleavage becomes predominant. Under identical conditions selectivity is also influenced by dispersion. If we accept that oxygen bonded reversibly to the surface platinum atom is a measure for metallic

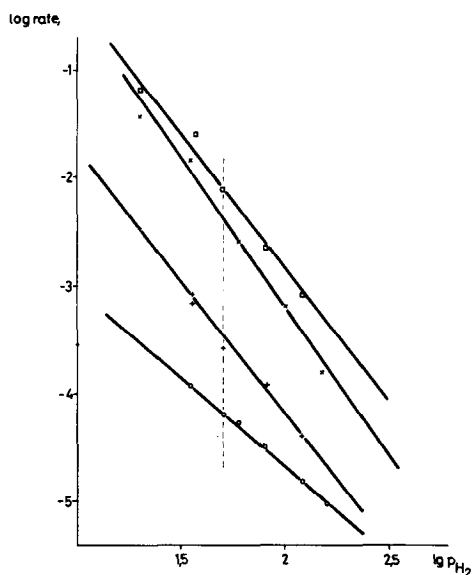


FIG. 5. Activity vs hydrogen pressure in the hydrogenolysis of ethane at different iron contents: (x) 0 atom% Fe; (□), 25 atom% Fe; (+), 41 atom% Fe; (○), 71 atom% Fe.

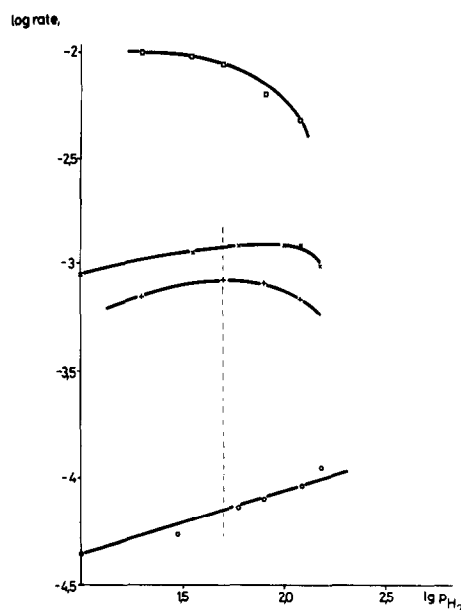


FIG. 6. Activity vs hydrogen pressure in the hydrogenolysis of *n*-butane at different iron contents (for symbols see legend to Fig. 5).

dispersion, the selectivity vs dispersion is plotted in Fig. 7 (the lowest *D* value refers to platinum black). *n*-Butane selectivity as a function of iron content is presented in Fig. 8.

4. DISCUSSION

4.1. Structure of the Catalytic Surface

TG-MS data (14) on silica gel containing platinum tetrammine complex and ferric nitrate have given rather strong evidence that even prior to the standard treatment the two metals in ionic form occupy neighboring sites on the surface. The complex is firmly held via Pt-O-Si bonds (19) and the reaction between NH₃ ligands and NO₃⁻ ions during the calcination takes place only if ferric nitrate is located in the vicinity of platinum complex. The necessity of metallic compounds being next to each other prior to the formation of the metallic phase is supported by the resemblance of catalytic properties between Pt/SiO₂ and a physical mixture of Pt/SiO₂ and Fe/SiO₂.

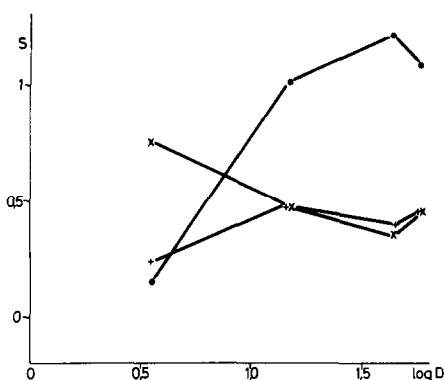


FIG. 7. Selectivity of *n*-butane hydrogenolysis vs metallic dispersion (*D*) calculated by equations $S_{C_i} = (4C_i / \sum_{i=1}^4 i C_i)$. (×), S_{C_1} ; (●), S_{C_2} ; (+), S_{C_3} ; (Δ), S_{C_4} .

The interaction between the two metals after reduction has been proved by Mössbauer spectroscopy (15). At low iron loading ($\text{Fe/Pt} < 1$) all iron atoms are reduced. Iron atoms, therefore, behave as if they were inserted into platinum matrix. Moreover, the positive isomer shift measured indicates the formation of a highly dispersed Pt-Fe compound and on the basis of the rigid band model this means that *s* electrons from iron are drifted to platinum. The corresponding effect has been observed for $^{195}\text{Pt-Fe}$ alloys (20), i.e., the negative isomer shift found indicated the increase of *s*-electron density at platinum nuclei.

However, if we accept the idea put forward by Qaim (21), iron in the Pt-Fe system has a larger electron density because of the enhanced overlapping of the *d* bands; consequently, due to its larger screening, *s*-electron density decreases at the Fe nucleus. This results in a net *d*-electron drift from platinum to iron and indeed a similar effect has been measured by ESCA for PtMo/SiO₂ (22), PtW/SiO₂ (23), and PtRe/Al₂O₃ (24). This idea is, in fact, in agreement with the model of "coherent potential approximation" which has been successfully used for, e.g., Ni-Cu and Pd-Ag systems (25). Indeed, a decrease in occupancy of *d* bands at platinum

and simultaneously an increase at iron may be expected if the UPS spectra for Pt (Ref. 2 in (26)) and for Fe (27) are compared. Of course, on the basis of Mössbauer spectroscopy alone we cannot decide whether *s*- or *d*-electron transfer is operative but this system has not been investigated by the ESCA method.

At high iron content ($\text{Fe/Pt} > 1$) iron above the stoichiometric ratio cannot be reduced. The main difference between catalysts with low and high iron load is that in the latter case a single peak with $\delta = 0$ mm/sec, and not PtFe with $\delta = 0.34$ mm/sec can be obtained which is due to either nonalloyed iron or to a combination of Pt-Fe and Fe⁰. Here we argue for the latter case based upon the evidence resulting from the reversibility in hydrogen reduction of the oxidized form at room temperature. This appears to be direct evidence for contact between iron and platinum because ferric oxide in high dispersion cannot be converted into Fe⁰ in absence of platinum.

At high iron loading the room temperature oxidation of reduced catalyst reveals

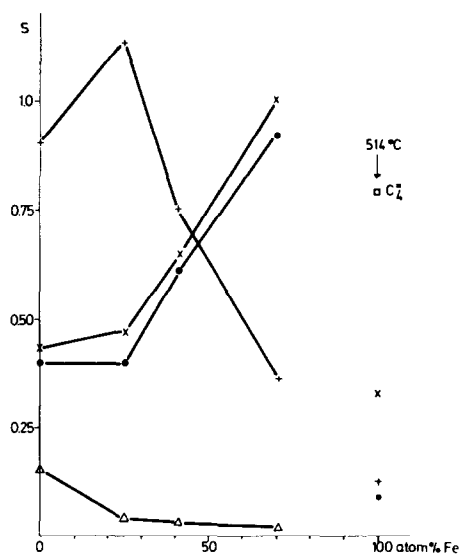


FIG. 8. Change of selectivity vs Fe content in *n*-butane hydrogenolysis. (×), S_{C_1} ; (+), S_{C_2} ; (●), S_{C_3} ; (Δ), S_{C_4} .

all iron as Fe^{3+} , indicated by the high-spin ferric doublet (15). This means that most of the iron is sitting on the surface or occupies the uppermost layers, mainly surrounded by iron and only a small fraction of platinum is inserted into the iron matrix.

Chemisorption results can be readily interpreted on the basis of the Mössbauer experiments. Since at low iron loading only a fraction of the iron is at the surface the increase of adsorption is mainly ascribed to an increase in the number of surface metal atoms, regardless of whether it is Pt or Pt-Fe. This observation agrees well with the results obtained by Engels and co-workers (8, 9) for the supported and unsupported platinum-iron system.

At iron loading above 41 atom% the surface contains Fe^0 , Fe-Pt, Fe^{3+} and Fe^{2+} . The last two species are not involved in the chemisorption process. Pt-Fe behaves as in low iron loading but a part of the Fe^0 oxidized at room temperature cannot be reduced by hydrogen at room temperature but only at 773 K. This means that this part is not in direct contact with platinum and hydrogen is available only after high-temperature activation. If we accept this picture the ideas of Bartholomew and Boudart (5) for Pt-Fe on carbon and Bolivar *et al.* (28) for Pt-Re/alumina can be applied to estimate the fraction of iron not alloyed with platinum. Namely, on oxygen adsorption all surface atoms can be covered but on hydrogen titration only the iron which is alloyed with platinum can be recovered. Taking the data presented in Table 3 for catalyst E, there is $7.6 \mu\text{mol}/\text{g}_{\text{cat}}$ iron (calculated from the irreversible adsorption) which is not alloyed and about $1.5 \mu\text{mol}/\text{g}_{\text{cat}}$ iron is associated with platinum. Consequently, the nominal Pt/Fe = 1 ratio (considering only the fraction which can be reduced) drops to Pt/Fe = 0.14 and may be even lower.

4.2. Correlation between Surface Structure and Catalytic Activity

From the exchange experiments of ethane carried out either separately or along with hydrogenolysis we may establish that the mechanism of hydrogenolysis is unchanged in the whole iron concentration range, i.e., adsorption of reactant is faster than C-C bond rupture on the catalyst surface (29).

The effect of Pt-Fe interaction becomes quite clear if the catalytic activity of a physical mixture (catalyst F) and that of Fe/SiO₂ (catalyst G) are compared. In the former case the activity pattern is similar to that of Pt/SiO₂ while in the latter case the catalytic activity is about three orders of magnitude lower than for catalyst E.

A possible reason for the inactivity of iron is given by Anderson (30) who proposed that under UHV conditions the iron film is covered by highly dehydrogenated hydrocarbon residues which to a large extent block the active sites. Conversely, carbonaceous deposits can be formed if a sufficient amount of hydrogen is not available on the surface. This latter case may be valid if we consider that hydrogen chemisorption on iron is negligible. This is the reason for the positive hydrogen order found by Sinfelt (31) only for iron among the Group VIII metals.

At low iron loading an increase in the number of surface metal atoms results in an increase of the rate of hydrogenolysis, leaving the energy of activation and the order of reaction w.r.t. hydrogen practically unchanged. This is supported by the effect of small amounts of iron on the selectivity of ethane formation, which reveals the same trend as in the case of the increase of dispersion (compare Figs. 7 and 8).

Experimental observations concerning energy of activation, hydrogen order, and selectivity obtained for the catalyst with high iron content make this catalyst similar

TABLE 4
Selectivity Patterns for *n*-Butane Hydrogenolysis^a

Condition	Multiple	Statistical	Middle	Terminal
	$S_{C_1} \gg S_{C_2} > S_{C_3}$	$S_{C_1} \sim S_{C_2} \sim S_{C_3}$	$S_{C_2} \gg S_{C_1} \sim S_{C_3}$	$S_{C_1} \simeq S_{C_3} \gg S_{C_2}$
Temperature	A ←————→ C			
	B ←————→			
Hydrogen pressure	A —————→		←————→ C	
	B —————→			
Activity	A —————→		←————→ C	
	B —————→			
Dispersity		—————→ C		
Alloying with iron			—————→ C	

^a (A) Massive Pt; (B) massive Ni; (C) supported Pt. For selectivity definition, see legend to Fig. 7.

to nonnoble transition metals, e.g., Ni (29), Fe (31), and Co (32).

It is therefore plausible to assume that the active sites on catalyst *E* are iron atoms modified by the presence of platinum. This latter can supply the amount of hydrogen which is necessary for hydrogenolysis. This is supported by the following experimental facts: energy of activation similar to that measured on iron,

order of reaction w.r.t. hydrogen between those measured on Pt/SiO₂ and Fe/SiO₂, TPD measurement which shows that in catalyst *E* hydrogen with medium strength is also available whereas there is no hydrogen chemisorption on Fe/SiO₂.

The explanation given above is confirmed by the selectivity data. In Table 4 all possible selectivity patterns are summarized. The arrows in the table show the direction of changes in selectivity under the effect of the parameters indicated in column 1. Earlier it was shown (18) that for active platinum black multiple C-C bond rupture was predominant, yielding mostly methane. On Pt/SiO₂ the middle C-C bond splitting is the main pathway. The effect of a temperature increase is to enhance S_{C_1} and S_{C_2} for Pt and Pt/SiO₂, respectively. This is an essential difference and to a first approximation this may be ascribed to the dispersion effect (see Fig. 7). On both types of catalyst the selectivity pattern is shifted to statistical distributions as a result of increasing hydrogen pressure or of decreasing catalytic activity. On the other hand, at high iron loading the selectivity pattern points to terminal C-C bond rupture. This is characteristic of a nickel catalyst with low activity. Again

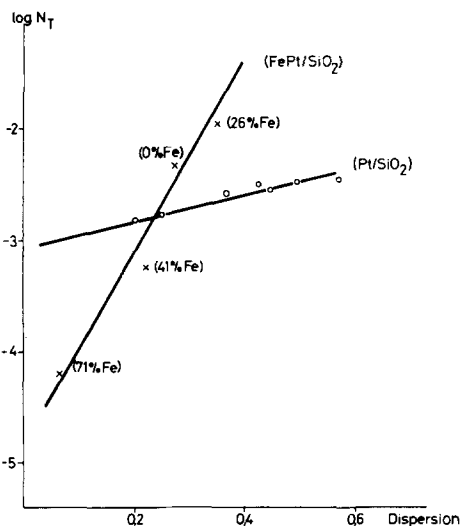


FIG. 9. Turnover number (N_t) vs metallic dispersion (D) in ethane hydrogenolysis for Pt/SiO₂ and FePt/SiO₂ catalysts.

we see properties of nonnoble transition metals, and this gives strong evidence that at high iron loading the catalytic pattern is determined by iron itself.

Finally, we wanted to find out whether the demanding character of the hydrogenolysis on iron-containing catalyst is the same as on pure platinum (33 to 35). In Fig. 9 the turnover number (N_i) for ethane hydrogenolysis on Pt/SiO₂ (35) is seen to have a different slope from that measured on PtFe/SiO₂ in the present work. This means that the addition of iron to platinum reveals some modification of the active sites in addition to the dispersion effect which is mainly operative on catalysts containing small amounts of iron.

CONCLUSIONS

(i) TG-MS and Mössbauer data along with gas adsorption give evidence for metallic interaction between iron and platinum prior to and after standard treatment. In both cases the catalysts prepared are well dispersed. At least a fraction of the iron can be oxidized and reduced at room temperature pointing to a direct contact between the two metals.

(ii) Catalyst activity passes through a maximum with increase in Fe content and the alloy activity is higher than those for the pure metals. Proceeding from low to high iron loading the amount of hydrogen which is easily available for reaction decreases; thus the hydrogen order increases and this result in a shift to less negative values in the reaction order with respect to hydrogen.

(iii) Based upon selectivity data at low iron loading the main effect is the enhancement in dispersion of platinum at the surface. At higher iron contents the iron gradually takes over the role of catalytic activity. In this range platinum supplied active hydrogen atoms to the reaction occurring at iron sites. It is believed that

the electron interaction between the two metals plays marginal role in the catalysis.

ACKNOWLEDGMENTS

We are indebted to Professor V. Ponec for valuable discussions and the late Dr. D. Móger for the evaluation of TPD measurements.

REFERENCES

1. Sachtler, W. M. H., *Am. Chem. Soc. Div. Pet. Chem.*, Preprint, 1976.
2. Ponec, V., *Catal. Rev.* **11**, 41 (1975).
3. Sinfelt, J. H., *J. Catal.* **29**, 308 (1973).
4. Clarke, J. K. A., *Chem. Rev.* **74** (3), 291 (1975).
5. Bartholomew, C. H., and Boudart, M., *J. Catal.* **29**, 278 (1973).
6. Garten, R. L., and Ollis, D. F., *J. Catal.* **35**, 232 (1974).
7. Garten, R. L., "Mössbauer Effect Methodology," Vol. 10, 1976.
8. Engels, S., Mörke, W., and Siedler, J., *Z. Anorg. Allg. Chem.* **431**, 181 (1977).
9. Engels, S., Mörke, W., and Siedler, J., *Z. Anorg. Allg. Chem.* **431**, 191 (1977).
10. Engels, S., and Siedler, J., *Z. Chem.* **17**, 150 (1977).
11. Vannice, M. A., and Garten, R. L., *J. Molec. Catal.* **1**, 201 (1976).
12. Derouane, E. G., LoJacono, M., Schiavello, M., and Cimino, A., *J. Phys. Chem.* **75**, 1044 (1971).
13. Benesi, H. A., Curtis, M. P., and Studer, J., *J. Catal.* **10**, 328 (1969).
14. Guzzi, L., Matusek, K., Margitfalvi, J., Eszterle, M., and Till, F., *Acta Chim. Acad. Sci. Hung.*, in press.
15. Dézsi, I., Nagy, D. L., Eszterle, M., and Guzzi, L., *React. Kinet. Catal. Lett.* **8**, 301 (1978).
16. Mears, D. E., and Hansford, R. C., *J. Catal.* **9**, 125 (1967); Wilson, G. R., and Hall, W. K., *J. Catal.* **17**, 190 (1970); Benson, J. E., Hwang, H. S., and Boudart, M., *J. Catal.* **30**, 146 (1973).
17. Yao, H. C., and Shelef, M., *J. Catal.* **43**, 392 (1976).
18. Guzzi, L., Sárkány, A., and Tétényi, P., *J. Chem. Soc. Faraday Trans. I* **70**, 1971 (1974).
19. Anderson, J. R., "Structure of Metallic Catalysts," Academic Press, New York, 1975.
20. Agresti, D., Kankleit, E., and Persson, B., *Phys. Rev.* **155**, 1339 (1967).
21. Qaim, S. M., *Proc. Phys. Soc.* **90**, 1065 (1967).
22. Yermakov, Yu. I., Kuznetsov, B. N., and Ryndin, Yu. A., *J. Catal.* **42**, 73 (1976).

23. Ioffe, M. S., Kuznetsov, B. N., Ryndin, Yu. A., and Yermakov, Yu. I., "Proc. 6th Int. Congress on Catalysis (London 1976)," p. 131. Chemical Society, London, 1977.
24. von Meerwall, E., and Schreiber, D. S., *Phys. Rev. B* **3**, 1 (1971).
25. Dev, B., and Ulmer, K., *Solid State Commun.* **20**, 139 (1976).
26. Lin, S. F., Pierce, D. T., and Spicer, W. E., *Phys. Rev. B* **4**, 326 (1971).
27. Duff, K. J., and Das, T. P., *Phys. Rev. B* **3**, 192 (1971).
28. Bolivar, C., Charcosset, H., Frety, R., Primet, M., Tournayan, L., Betizeau, C., Leclercq, G., and Maurel, R., *J. Catal.* **45**, 163 (1976).
29. Guzzi, L., Gudkov, B. S., and Tétényi, P., *J. Catal.* **24**, 187 (1972).
30. Anderson, J. R., "Chemisorption and Reaction on Metallic Films," Vol. 2. Academic Press, New York/London, 1971.
31. Sinfelt, J. H., *Advan. Catal.* **23**, 91 (1973).
32. Babernics, L., Guzzi, L., Matusek, K., Sárkány, A., and Tétényi, P., "Proc. 6th Int. Congress on Catalysis (London 1976)," p. 456, Chemical Society, London, 1977.
33. Boudart, M., *Advan. Catal.* **20**, 153 (1969).
34. Brunelle, J. P., Sugier, A., and Le Page, J. F., *J. Catal.* **43**, 273 (1976).
35. Guzzi, L., and Gudkov, B. S., *React. Kinet. Catal. Lett.*, **9**, 343 (1978).